

A Kinetic Analysis of the Initial Stages of the Sol–Gel Reactions of Methyltriethoxysilane (MTES) and a Mixed MTES/Tetraethoxysilane System by High-Resolution ^{29}Si NMR Spectroscopy

Colin A. Fyfe* and Patricia P. Aroca

Department of Chemistry, University of British Columbia, Vancouver, B.C., Canada V6T 1Z1

Received: May 9, 1997[⊗]

^{29}Si solution NMR is used to follow the kinetics of the methyltriethoxysilane (MTES) homopolymerization and that of the MTES/tetraethoxysilane (TEOS) copolymerization. Individual kinetic rate constants for the hydrolysis and dimerization reactions were obtained by fitting the concentration curves as functions of time for the different intermediate species. It was found that the individual hydrolysis kinetic constants for the MTES homopolymerization are greater than those for the TEOS homopolymerization. Using the homodimerization and codimerization kinetic rate constants for the MTES/TEOS copolymerization, reactivity ratios were calculated. These reactivity ratios suggest that the two monomers react to form a random copolymer.

Introduction

Organofunctionalized silicas and silica gels have a wide variety of applications. They are used for the immobilization of expensive catalyst or toxic materials,¹ in column chromatography,² as adhesion promoters,³ and in numerous other industrial applications.³ Traditionally, the preparation of organofunctionalized silica gels has involved the condensation of a functionalized trichloro- or trialkoxysilane onto the surface of solid silica gel. However, the presence of water favors not only surface but self-condensation of the functionalized silane, resulting in the formation of siloxane oligomers. To bypass this problem, organofunctionalized silica gels can be synthesized by a copolymerization of the organofunctionalized silane and tetraethoxysilane monomers. Solid-state NMR studies on organofunctionalized silica gel samples prepared via copolymerization of the two monomers have shown (1) that the functionality is intact in the final product and (2) that the two monomers are not phase separated.⁷

This paper presents further insight into the distribution of the functionality in the silica gel matrix by characterizing the kinetics of the copolymerization process, specifically the hydrolysis and dimerization reactions. The model copolymerization studied is that between methyltriethoxysilane (MTES) and tetraethoxysilane (TEOS) monomers. It was assumed in this approach that the dimerization reactions are typical of further condensation reactions involved in forming the gel. The homopolymerization kinetic rate constants were used as starting values for the determination of the kinetic constants in the copolymerization analysis. A detailed characterization of the TEOS homopolymerization process has already been published.⁴ This paper presents an analysis of the MTES homopolymerization and the MTES/TEOS copolymerization reactions.

Experimental Section

The composition of the reaction mixtures for the MTES homopolymerization studies was 1.36 M MTES, 7.81 M ethanol, 15.01 M water acidified with HCl, and 0.016 M chromium acetylacetonate ($\text{Cr}(\text{acac})_3$). The MTES homopolymerization was studied at a variety of pHs ranging from 2.45 to 3.35. The pH values quoted are those of the water added to the reaction mixture.

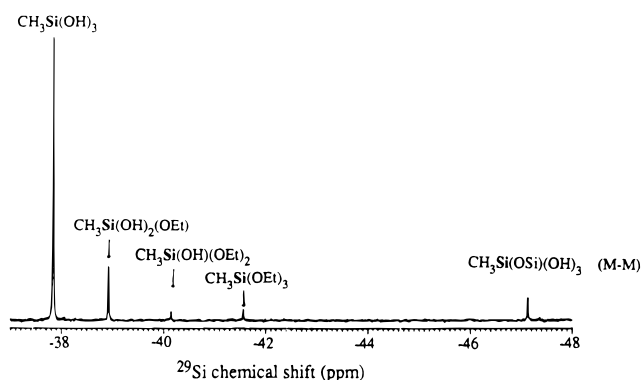


Figure 1. Typical ^{29}Si solution NMR spectrum obtained during the hydrolysis of methyltriethoxysilane (MTES) in water/ethanol with all the peaks assigned as indicated.

The composition of the reaction mixtures for the MTES/TEOS copolymerization studies differed only in that two monomers were involved in the reaction; 0.671 M TEOS and 0.671 M MTES were used. This reaction was studied at pH = 2.55.

All ^{29}Si NMR experiments were carried out in duplicate on a Bruker AMX 500 MHz spectrometer with a 10 mm broadband probe and a temperature control unit maintained at 300.0 ± 0.1 K. The T_1 values for all the intermediate hydrolysis species are very similar, and chromium acetylacetonate was added to lower the values to ~ 1.6 s. Eight scans were acquired for each spectrum with a 60° pulse on the ^{29}Si channel and gated decoupling on the ^1H channel. For the MTES homopolymerization studies the recycle delay was 0.8 s, and for the MTES/TEOS copolymerization study the recycle delay was 1 s. To follow the concentrations of the different species as functions of time a spectrum was acquired every 1.5–2 min. Enough spectra were acquired in order to accurately characterize the growth and decay of all the species up to the formation of the dimers.

Results and Discussion

A typical ^{29}Si spectrum obtained during the hydrolysis of methyltriethoxysilane is shown in Figure 1 with all the peaks labeled. An example of the time dependence of the spectra during the hydrolysis is shown in Figure 2. The relative concentration vs time curves for all the intermediate hydrolysis species were determined by integration over fixed individual

* Author to whom correspondence should be addressed.

[⊗] Abstract published in *Advance ACS Abstracts*, October 15, 1997.

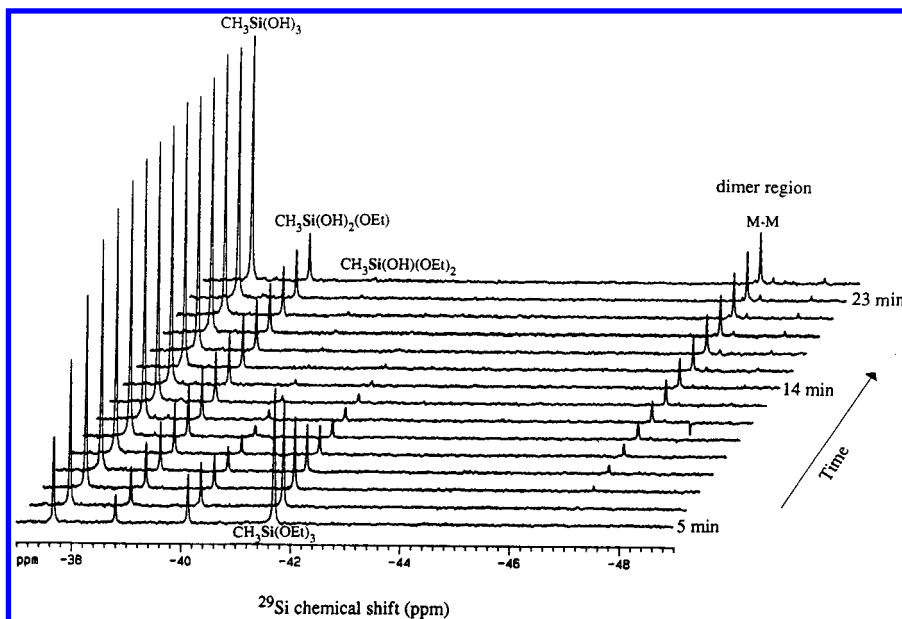
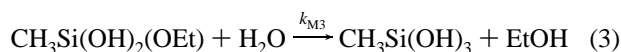
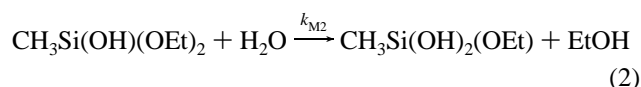


Figure 2. The time dependence of the 1D ^{29}Si solution NMR spectra during the polymerization of MTES at pH = 2.55.

frequency ranges in the spectra. The total integrated area for the initial ^{29}Si spectrum was taken to be 100%. The experimental conditions were chosen such that the hydrolysis and condensation reactions were well separated. Experimentally this was confirmed by the fact that the majority of the MTES monomer was fully hydrolyzed before any dimers were formed. For example, in the MTES homopolymerization at pH = 2.55, there is a clear differentiation between the hydrolysis and condensation reactions, i.e. at 20 min approximately 95% of the silicons are present in either $\text{CH}_3\text{Si}(\text{OEt})(\text{OH})_2$ or $\text{CH}_3\text{Si}(\text{OH})_3$ and about 5% in the dimer form. In the analysis of the experimental data, the time period used in the fitting procedures is that up to the first indications of higher oligomer formation. In many cases the fitting is very good for the longer time periods since the formation of higher oligomers under these conditions is relatively slow.

In the analysis of the MTES homopolymerization, four reactions (1–4) were used to fit the concentration curves of the hydrolysis intermediates.



Explicit equations can be written for the change in concentration as a function of time for the intermediate species $\text{CH}_3\text{Si}(\text{OEt})_3$ to $\text{CH}_3\text{Si}(\text{OH})_2(\text{OEt})$, assuming a constant water concentration ($[\text{H}_2\text{O}]$) and reactions 1–3 as forward reactions. The first step in the fitting of the experimental concentration vs time curves was to do a nonlinear least squares fitting, using these explicit expressions for the change in concentration of $\text{CH}_3\text{Si}(\text{OEt})_3$, $\text{CH}_3\text{Si}(\text{OH})(\text{OEt})_2$, and $\text{CH}_3\text{Si}(\text{OH})_2(\text{OEt})$. The experimental data used and the calculated curves obtained from this fit are shown in Figure 3. The calculated curve for the $\text{CH}_3\text{Si}(\text{OH})_2(\text{OEt})$ species is not a good approximation for the experimental data, indicating that the above assumptions are not valid for this species.

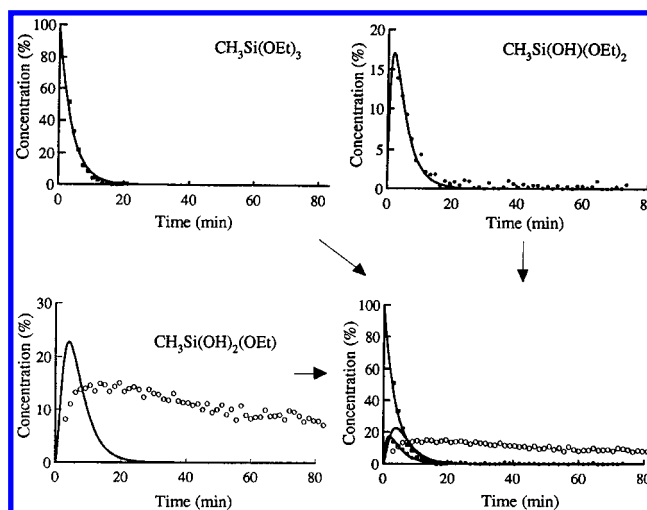


Figure 3. Calculated curves from the trial nonlinear least squares fitting of the time dependences of the percent concentrations of the intermediate species as indicated in the hydrolysis of MTES, assuming a constant water concentration, together with the experimental data, pH = 2.55. $\text{CH}_3\text{Si}(\text{OEt})_3$ (■), $\text{CH}_3\text{Si}(\text{OH})(\text{OEt})_2$ (●), $\text{CH}_3\text{Si}(\text{OH})_2(\text{OEt})$ (○).

In order to fit the $\text{CH}_3\text{Si}(\text{OH})_3$ data, the dimer formation reaction responsible for the decay of this species had to be included in the kinetic model. This change results in differential equations that are no longer explicitly solvable. These interdependent equations were solved numerically using a program called LSODE.⁸ The high water/silane ratio used in these reactions minimizes condensation between partially hydrolyzed species by favoring the hydrolysis process. No partially hydrolyzed dimers were detected during the time period that the reaction was studied, and therefore only the dimerization reaction between fully hydrolyzed monomers was considered in the model, reaction 4.

The next step was to try to improve the fit of the $\text{CH}_3\text{Si}(\text{OH})_2(\text{OEt})$ concentration vs time profile by including the change in water concentration. This had no significant effect on the shape of the calculated curves, as was observed previously in the TEOS homopolymerization study.⁴ The large water/silane and ethanol/silane ratios used (11 and 6, respectively) are probably responsible for the very small effect observed when the variation of water concentration was included. However, the change in water concentration was included in the final set of equations for completeness.

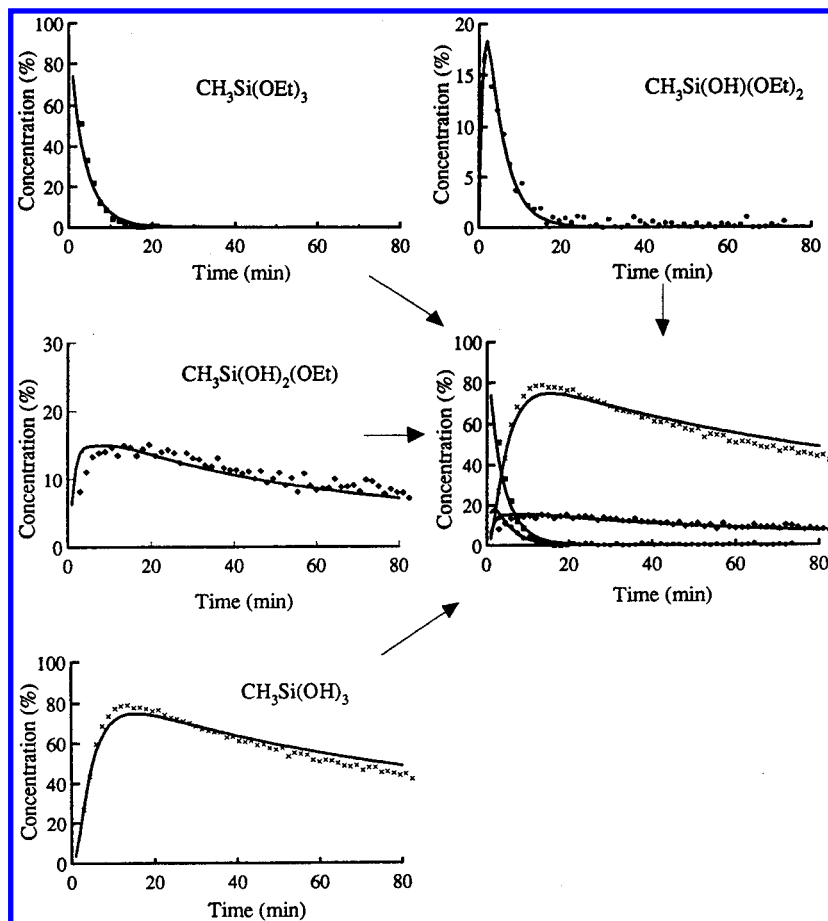


Figure 4. The time dependences of the percent concentrations of all the intermediate species involved in the hydrolysis of MTES together with the final calculated curves, pH = 2.55. $\text{CH}_3\text{Si}(\text{OEt})_3$ (■), $\text{CH}_3\text{Si}(\text{OH})(\text{OEt})_2$ (●), $\text{CH}_3\text{Si}(\text{OH})_2(\text{OEt})$ (◆), $\text{CH}_3\text{Si}(\text{OH})_3$ (×).

Experimentally, the $\text{CH}_3\text{Si}(\text{OH})_2(\text{OEt})$ data are characterized by a plateau after the maximum which undergoes minimal decay as the reaction proceeds, suggesting that an equilibrium exists between $\text{CH}_3\text{Si}(\text{OH})_2(\text{OEt})$ and $\text{CH}_3\text{Si}(\text{OH})_3$. The re-esterification reaction of $\text{CH}_3\text{Si}(\text{OH})_3$ was therefore included in the model in order to satisfactorily fit the concentration profile of $\text{CH}_3\text{Si}(\text{OH})_2(\text{OEt})$. This situation is analogous to that previously found for the TEOS homopolymerization where consideration of the re-esterification reaction of $\text{Si}(\text{OH})_4$ was essential to fit the $\text{Si}(\text{OH})_3(\text{OEt})$ concentration vs time profile.⁴

The final set of differential equations used in the fitting of the experimental data is summarized below.

$$\frac{d[\text{MTES}]}{dt} = -k_{M1}[\text{MTES}]_t \eta_t^m \quad (5)$$

$$\frac{d[\text{CH}_3\text{Si}(\text{OH})(\text{OEt})_2]}{dt} = (k_{M1}[\text{MTES}]_t - k_{M2}[\text{CH}_3\text{Si}(\text{OH})(\text{OEt})_2]_t) \eta_t^m \quad (6)$$

$$\frac{d[\text{CH}_3\text{Si}(\text{OH})_2(\text{OEt})]}{dt} = (k_{M2}[\text{CH}_3\text{Si}(\text{OH})(\text{OEt})_2]_t - k_{M3f}[\text{CH}_3\text{Si}(\text{OH})_2(\text{OEt})]_t \eta_t^m + k_{M3b}[\text{CH}_3\text{Si}(\text{OH})_3]_t \epsilon_t^m) \quad (7)$$

$$\frac{d[\text{CH}_3\text{Si}(\text{OH})_3]}{dt} = k_{M3f}[\text{CH}_3\text{Si}(\text{OH})_2(\text{OEt})]_t \eta_t^m - k_{M3b}[\text{CH}_3\text{Si}(\text{OH})_3]_t \epsilon_t^m - k_{M4}[\text{CH}_3\text{Si}(\text{OH})_3]_t^2 \quad (8)$$

where

$$\eta_t^m = [\text{H}_2\text{O}]_0 - [\text{CH}_3\text{Si}(\text{OH})(\text{OEt})_2]_t - 2[\text{CH}_3\text{Si}(\text{OH})_2(\text{OEt})]_t - 3[\text{CH}_3\text{Si}(\text{OH})_3]_t \quad (9)$$

$$\epsilon_t^m = [\text{EtOH}]_0 + [\text{CH}_3\text{Si}(\text{OH})(\text{OEt})_2]_t + 2[\text{CH}_3\text{Si}(\text{OH})_2(\text{OEt})]_t + 3[\text{CH}_3\text{Si}(\text{OH})_3]_t \quad (10)$$

The final calculated curves at pH = 2.55 are shown in Figure 4. It is anticipated that the calculated curve for $\text{CH}_3\text{Si}(\text{OH})_3$ well overestimates the decay at long reaction times as observed since some condensation of dimer species is beginning to occur. The maximum of $\text{CH}_3\text{Si}(\text{OH})_3$ is determined mainly by the re-esterification kinetic constant which also controls the decay of the $\text{CH}_3\text{Si}(\text{OH})_2(\text{OEt})$ species. Considering the complexity of the system, the overall fit of the data is considered to be quite good. The pH-dependent kinetic constants obtained for different catalysis concentrations are summarized in Table 1. A plot of the pH-dependent kinetic constants as a function of the acid concentration gives the pH-independent kinetic constants summarized in Table 2 together with those previously obtained for the homopolymerization of TEOS.⁴

The data in Table 2 provide the first quantitative evidence that each of the individual hydrolysis kinetic constants is greater for the MTES homopolymerization than those for the TEOS homopolymerization. This is in agreement with the qualitative conclusion in the literature that alkyl-substituted trialkoxysilanes hydrolyze faster than the corresponding tetraalkoxysilane.^{5,6}

For both the MTES and TEOS homopolymerizations the rate of hydrolysis increases with the number of hydroxyls for the first three sequential hydrolysis rate constants, $k_1 < k_2 < k_3$. For both the MTES and TEOS, the dimer formation is slower than the last hydrolysis, $k_{T4f} > k_{T5}$ (TEOS) and $k_{M3f} > k_{M4}$ (MTES), so that at all pH values studied there is an accumulation

TABLE 1: Average pH-Dependent Kinetic Rate Constants ($M^{-1} \text{ min}^{-1}/1000$) Determined for Hydrolysis and Dimer Formation Reactions in the MTES Homopolymerization^a

pH	k_{M1}	k_{M2}	k_{M3f}	k_{M3b}	k_{M4}
3.35	1.5 ± 0.3	6 ± 1	8.5 ± 0.5	0.5 ± 0.1	1 ± 0.2
3.04	5.2 ± 0.2	19 ± 5	23 ± 5	1 ± 0.5	5 ± 0.5
2.88	6 ± 1	24 ± 5	35 ± 5	3.5 ± 0.5	6 ± 0.5
2.76	13 ± 1	45 ± 5	50 ± 5	4 ± 0.5	7 ± 0.5
2.55	20.5 ± 0.5	65.5 ± 0.5	70 ± 2	8 ± 3	17 ± 4
2.45	25 ± 0.5	75 ± 5	85 ± 5	10 ± 2	21.5 ± 0.5

^a Error estimated from the variation in the fitting of duplicate data sets.

TABLE 2: Values of the pH-Independent Kinetic Rate Constants (min^{-1}) for the MTES and TEOS⁴ Hydrolysis and Dimer Formation Reactions Together with the Estimated Errors^a

kinetic constants	MTES homopolymzn (min^{-1})	TEOS homopolymzn (min^{-1})
k_{M1}, k_{T1}	25 ± 1	3.3 ± 0.1
k_{M2}, k_{T2}	81 ± 3	18 ± 1
k_{M3f}, k_{T3}	91 ± 2	72 ± 5
k_{M3b}	9.9 ± 0.7	
k_{T4f}		59 ± 10
k_{T4b}		11 ± 2
k_{M4}, k_{T5}	21 ± 1	51 ± 2

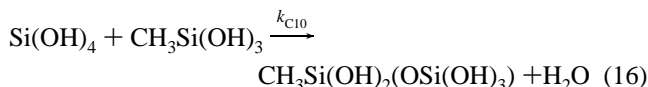
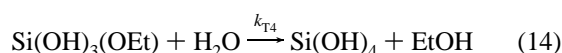
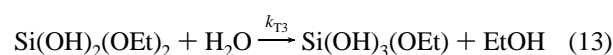
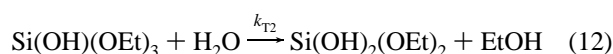
^a Estimated errors are taken as the standard error from the fit of all the pH-dependent values.

of the fully hydrolyzed monomers. Interestingly, the homodimer formation kinetic constant is greater for TEOS than MTES homopolymerization. In addition, both the MTES and TEOS homopolymerization studies require the inclusion of a re-esterification reaction for the last hydrolysis in order to respect the general shape of the second to last hydrolysis product concentration vs time curve. This re-esterification reaction is smaller in both cases than the forward hydrolysis reaction by at least a factor of 5, i.e. $k_{T4f} \gg k_{T4b}$ (TEOS) and $k_{M3f} \gg k_{M3b}$ (MTES).

MTES/TEOS Copolymerization

A typical 1D spectrum obtained during the MTES/TEOS copolymerization is shown in Figure 5. Resonances for the thirteen hydrolysis and dimer species are resolved in the spectra, and their concentrations can be monitored simultaneously as functions of time.

In an analogous manner to that described for the MTES monomer, the concentration profiles were obtained for all the intermediate hydrolysis species. The kinetic model for the MTES/TEOS copolymerization involves reactions 1–4 for the MTES monomer and reactions 11–15 listed below involving the TEOS monomer and the condensation reaction 16 involving both monomers.



The composition of the MTES/TEOS copolymerization reaction mixture was chosen such that the water/(total silane) and acid/(total silane) ratios were equal to those of the homopolymerizations previously studied. Due to the presence of two monomers, the water/(total silane) and water/TEOS or

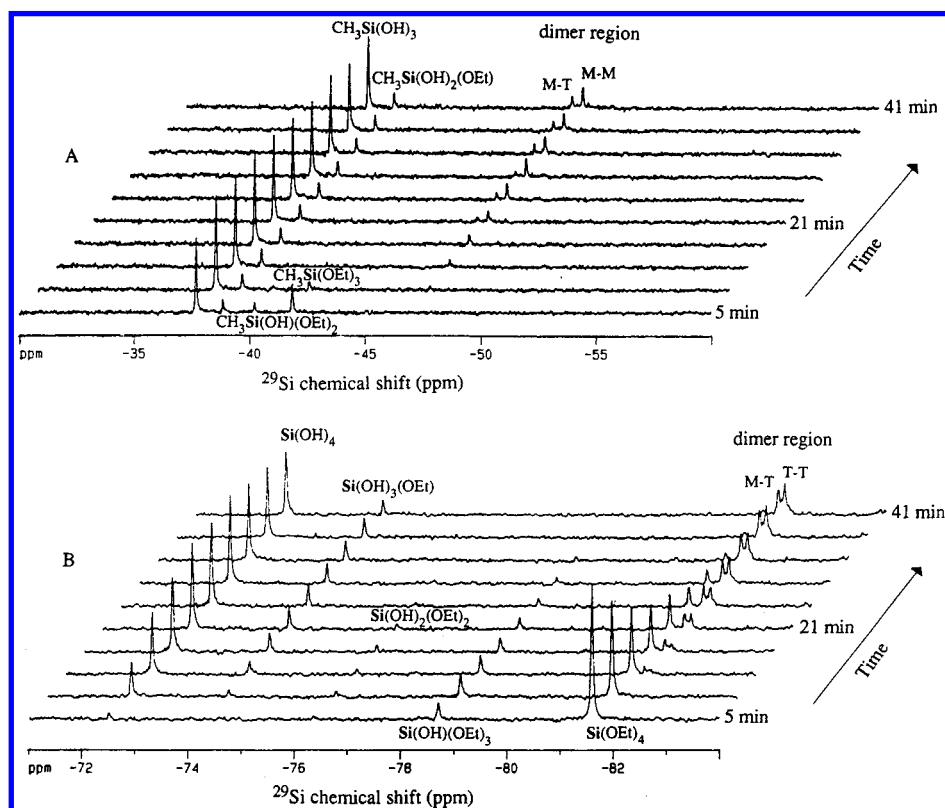


Figure 5. A typical example of the time dependence of the 1D ^{29}Si solution NMR spectra for the copolymerization of MTES and TEOS at pH = 2.55. A: MTES shift region. B: TEOS shift region.

water/MTES cannot be the same as in the homopolymerization studies, and therefore it is not expected that exactly the same kinetic constants will characterize the corresponding reactions in both homopolymerization and copolymerizations. As in the homopolymerization studies, negligible concentrations of non-fully hydrolyzed dimers were observed during the reaction time studied, supporting omission of condensation reactions between partially hydrolyzed monomers in the model.

For eleven out of the twelve copolymerization kinetic rate constants sought, reasonable starting values are available from the previous homopolymerization studies. The differential equations used to fit the complete collection of data for all the hydrolysis intermediates in the MTES/TEOS copolymerization are interdependent and not explicitly solvable. These equations include the change in water and ethanol concentration, three dimerization reactions (4, 15, and 16), and two re-esterification reactions (3 and 14). The equations used to fit the copolymerization data are given below:

$$\frac{d[\text{TEOS}]}{dt} = -k_{T1}[\text{TEOS}]_t \eta_t^c \quad (17)$$

$$\frac{d[\text{Si(OH)(OEt)}_3]}{dt} = (k_{T1}[\text{TEOS}]_t - k_{T2}[\text{Si(OH)(OEt)}_3]_t) \eta_t^c \quad (18)$$

$$\frac{d[\text{Si(OH)}_2(\text{OEt})_2]}{dt} = (k_{T2}[\text{Si(OH)(OEt)}_3]_t - k_{T3}[\text{Si(OH)}_2(\text{OEt})_2]_t) \eta_t^c \quad (19)$$

$$\frac{d[\text{Si(OH)}_3(\text{OEt})]}{dt} = (k_{T3}[\text{Si(OH)}_2(\text{OEt})_2]_t - k_{T4f}[\text{Si(OH)}_3(\text{OEt})]_t \eta_t^c + k_{T4b}[\text{Si(OH)}_4]_t \epsilon_t^c) \quad (20)$$

$$\frac{d[\text{Si(OH)}_4]}{dt} = k_{T4f}[\text{Si(OH)}_3(\text{OEt})]_t \eta_t^c - k_{T4b}[\text{Si(OH)}_4]_t \epsilon_t^c - k_{T5}[\text{Si(OH)}_4]_t^2 - k_{C10}[\text{CH}_3\text{Si(OH)}_3]_t[\text{Si(OH)}_4]_t \quad (21)$$

$$\frac{d[\text{MTES}]}{dt} = -k_{M1}[\text{MTES}]_t \eta_t^c \quad (22)$$

$$\frac{d[\text{CH}_3\text{Si(OH)(OEt)}_2]}{dt} = (k_{M1}[\text{MTES}]_t - k_{M2}[\text{CH}_3\text{Si(OH)(OEt)}_2]_t) \eta_t^c \quad (23)$$

$$\frac{d[\text{CH}_3\text{Si(OH)}_2(\text{OEt})]}{dt} = (k_{M2}[\text{CH}_3\text{Si(OH)(OEt)}_2]_t - k_{M3f}[\text{CH}_3\text{Si(OH)}_2(\text{OEt})]_t \eta_t^c + k_{M3b}[\text{CH}_3\text{Si(OH)}_3]_t \epsilon_t^c) \quad (24)$$

$$\frac{d[\text{CH}_3\text{Si(OH)}_3]}{dt} = k_{M3f}[\text{CH}_3\text{Si(OH)}_2(\text{OEt})]_t \eta_t^c - k_{M3b}[\text{CH}_3\text{Si(OH)}_3]_t \epsilon_t^c - k_{M4}[\text{CH}_3\text{Si(OH)}_3]_t^2 - k_{C10}[\text{CH}_3\text{Si(OH)}_3]_t[\text{Si(OH)}_4]_t \quad (25)$$

where

$$\eta_t^c = [\text{H}_2\text{O}]_0 - [\text{CH}_3\text{Si(OH)(OEt)}_2]_t - 2[\text{CH}_3\text{Si(OH)}_2(\text{OEt})]_t - 3[\text{CH}_3\text{Si(OH)}_3]_t - [\text{Si(OH)(OEt)}_3]_t - 2[\text{Si(OH)}_2(\text{OEt})_2]_t - 3[\text{Si(OH)}_3(\text{OEt})]_t - 4[\text{Si(OH)}_4]_t \quad (26)$$

TABLE 3: Comparison of the pH-Dependent Kinetic Rate Constants Determined for the TEOS and MTES Homopolymerizations and MTES/TEOS Copolymerization at pH = 2.55^a

	homopolymer results/100	copolymer results/100
TEOS		
k_{T1}	0.18 ± 0.002	0.6 ± 0.02
k_{T2}	1.1 ± 0.2	2.8 ± 0.2
k_{T3}	$6^b \pm 2$	$6^b \pm 2$
k_{T4f}	5 ± 0.5	10 ± 1
k_{T4b}	0.9 ± 0.1	2 ± 0.2
k_{T5}	3.3 ± 0.1	5 ± 0.5
MTES		
k_{M1}	2.1 ± 0.2	3.4 ± 0.2
k_{M2}	6.6 ± 0.2	8.5 ± 0.2
k_{M3f}	7 ± 0.5	10 ± 1
k_{M3b}	1 ± 0.2	2.5 ± 0.2
k_{M4}	2.1 ± 0.1	4 ± 0.2
Codimer		
k_{C10}		5 ± 0.5

^a The error stated is estimated from the variation in the calculated curve which still gives an acceptable fit to the experimental data. ^b No change in this case.

$$\epsilon_t^c = [\text{EtOH}]_0 + [\text{CH}_3\text{Si(OH)(OEt)}_2]_t + 2[\text{CH}_3\text{Si(OH)}_2(\text{OEt})]_t + 3[\text{CH}_3\text{Si(OH)}_3]_t + [\text{Si(OH)(OEt)}_3]_t - 2[\text{Si(OH)}_2(\text{OEt})_2]_t + 3[\text{Si(OH)}_3(\text{OEt})]_t + 4[\text{Si(OH)}_4]_t \quad (27)$$

The calculated curves obtained from the numerical solution to the above differential equations, using the homopolymerization kinetic constants and a negligible codimerization kinetic rate constant, do not fit the copolymerization experimental data exactly, as was anticipated from the change in the nature of the solution. Therefore, each kinetic constant was optimized on the corresponding data set in a sequential manner starting with k_{T1} , and k_{M1} . Larger errors are associated with the kinetic constants determined from the concentration profiles of species with low maxima. This is compensated by the fact that every kinetic constant is determined by the fitting of two curves, the decay of the reactant and the growth of the product.

The optimized copolymerization kinetic constants are summarized in Table 3, and the calculated curves are shown in Figure 6. The $\text{Si(OEt)}_2(\text{OH})_2$ data are not shown in Figure 6 because the maximum is in the range of 3% which is close to the experimental variation of the data. Nevertheless, the calculated curve does fit the data well, that is, the curve maximum and its shape are in accordance with what is observed.

A preliminary study on the effect of water on the initial hydrolysis of TEOS suggests that as the water/TEOS ratio increases, the rate of the first hydrolysis decreases, and therefore the variation of k_{T1} cannot be explained by the altered water/TEOS ratio in the copolymer case vs the homopolymer case. One possible explanation for the variation in k_{T1} (refer to Table 3) is the effect of the MTES monomer on the solution properties, such as polarity and viscosity, which inevitably affects the TEOS–water interaction.

In general, the kinetic constants obtained for the formation of the different dimers are not unique solutions to the fitting of the experimental data. However, other solutions can be eliminated because they do not reflect the ratios observed for the different dimers present in the reaction medium as functions of time. Estimates for the reactivity ratios for $\text{CH}_3\text{Si(OH)}_3$ or Si(OH)_4 were calculated by dividing the homodimer kinetic constants by the codimer kinetic rate constant (k_{C10}) as in 28.

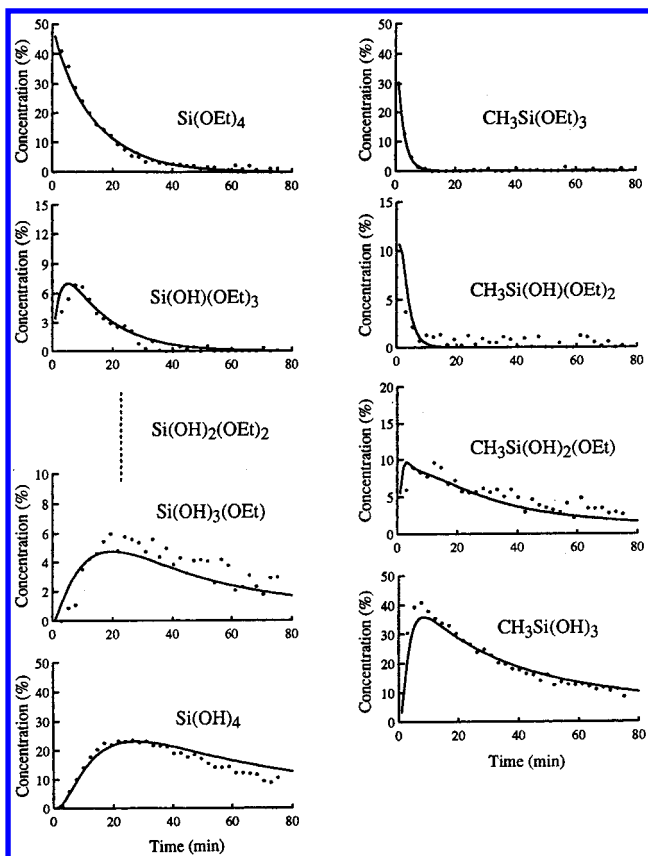


Figure 6. The time dependence of the percent concentrations of all the intermediate species involved in the mixed MTES/TEOS hydrolysis together with the final calculated curves, pH = 2.55. The kinetic rate constants used in the calculations are summarized in Table 3.

$$R_{\text{MTES}} = \frac{k_{\text{MTES-MTES}}}{k_{\text{MTES-TEOS}}} = \frac{k_{\text{M4}}}{k_{\text{C10}}}; \quad R_{\text{TEOS}} = \frac{k_{\text{TEOS-TEOS}}}{k_{\text{MTES-TEOS}}} = \frac{k_{\text{T5}}}{k_{\text{C10}}} \quad (28)$$

Using the data from Table 3, the reactivity ratios for MTES and TEOS are 0.80 ± 0.15 and 1.0 ± 0.2 , respectively. This suggests that the copolymerization of MTES and TEOS monomers tends to produce a random matrix if subsequent condensation reactions follow the same general trend. In fact, they are close enough to the ideal case that the copolymer composition should also approximate the reaction mixture composition which should remain constant. These results are in good agreement with previous solid-state NMR studies⁷ of the final gels where no evidence was found for any substantial phase separation of homopolymer volumes in the copolymer matrix.

Summary

The pH-dependent and -independent kinetic constants calculated for the hydrolysis and dimerization reactions of the

MTES homopolymerization provide the first quantitative evidence that the MTES monomer hydrolyzes faster than the TEOS monomer at each sequential hydrolysis reaction. These results imply that the methyl group stabilizes the transition state involved in the hydrolysis reactions. On the other hand, the MTES homopolymerization dimerization rate constant is slower than that for the TEOS monomer, suggesting that the methyl ligand destabilizes the transition state involved in the MTES/MTES homodimerization reaction. As in the TEOS homopolymerization, an equilibrium reaction was required in the model to respect the general shape of the concentration/time curve for the second to last hydrolysis intermediate, $\text{CH}_3\text{Si}(\text{OH})_2(\text{OEt})$.

Rate constants have been obtained for the first time for the MTES/TEOS copolymer hydrolysis and dimer formation reactions. In comparing the homopolymerization and copolymerization hydrolysis kinetic constants, it is evident that the TEOS monomer is significantly more affected than the MTES monomer by the presence of the other monomer. Reactivity ratios of 0.80 ± 0.15 and 1.0 ± 0.2 were calculated from the dimer formation kinetic rate constants for the MTES and TEOS monomers, respectively. These reactivity ratios suggest that the MTES/TEOS copolymerization tends to approximate a random copolymerization, producing a matrix with the methyl functionality randomly distributed, further supporting the data obtained by (1) the deconvolution of the dimer region of the spectrum and (2) previous solid-state NMR work done on this system.⁷ In conclusion, the copolymerization of a functionalized and a nonfunctionalized silane monomer results in a functionalized gel where the functionality is accessible for further reactions.

Acknowledgment. The authors acknowledge the financial assistance of NSERC of Canada in the form of Operating and Major Installation grants (C.A.F.) and the Defense Research Establishment (Pacific) (Contract W7708-0-0060). P.P.A. acknowledges the award of an NSERC Graduate Scholarship. We also thank Bruker Spectrospin (Canada) for advice and for the loan of the 10 mm broad-banded probe used in these studies.

References and Notes

- (1) Plueddeman, E. P. *Silane Coupling Agents*; Plenum Press: NY, 1982; p 333.
- (2) Chow, F. K.; Grushka, E. In *Silylated Surfaces*; Leyden, D. E., Collins, W. T., Eds.; Gordon & Breach Science Publishers Ltd.: NY, 1980; p 301.
- (3) Deschler, U.; Kleinschmidt, P.; Panster, P. *Angew. Chem., Int. Ed. Engl.* **1986**, 25, 236.
- (4) Fyfe, C. A.; Aroca, P. P. *Chem. Mater.* **1995**, 7 (10), 1800.
- (5) Andrianov, K. A. *Organic Silicon Compounds*; State Sci. Publ. House for Chemical Literature: Moscow, 1955.
- (6) Akeman, E. *Acta Chem. Scand.* **1956**, 10, 298; **1957**, 11, 298.
- (7) Fyfe, C. A.; Zhang, Y.; Aroca, P. P. *J. Am. Chem. Soc.* **1992**, 114, 3252.
- (8) Moore, C. *Systemized Collection of Ordinary Differential Equation Solvers*; UBC Computing Center: Canada, 1989.